A Spatial Decomposition Method for Solving the Security-Constrained Unit Commitment Problem

Arjun Kumar Madhusoodhanan*†, Marco Giuntoli‡, Susanne Schmitt‡, Iiro Harjunkoski‡,
Jan Poland‡, Thomas Leibfried†
* Institute of Automation and Applied Informatics, Karlsruhe Institute of Technology, Karlsruhe, Germany
arjun.madhusoodhanan@kit.edu
† Institute for Electrical Energy Systems and High Voltage Technology, Karlsruhe Institute of Technology, Karlsruhe, Germany
‡ Hitachi Energy Research, Mannheim, Germany

***Abstract*—Today, we are experiencing exponential growth in distributed energy sources and storage systems, such as Battery Energy Storage Systems (BESS), which participate in the day-ahead energy market. Moreover, the need for energy market coupling to ensure social welfare maximization and grid security makes the Security-Constrained Unit Commitment (SCUC) problem more challenging due to the increasing problem size. This work proposes a novel approach for solving the SCUC problem in a distributed manner by decomposing the grid into multiple areas connected by tie-lines. The solution leverages the Alternating Direction Method of Multipliers (ADMM) to solve the problem efficiently. The proposed Spatially Decomposed SCUC method significantly reduces the computational burden arising from the combinatorial nature of the problem. The speed-up and optimality of the proposed method is validated on the IEEE 118-bus and RTE 6468-bus systems.**

***Index Terms*—ADMM, Decomposition method, Parallel computing, Security constraints, Unit Commitment.**

I. Introduction

Europe aims to become the first climate-neutral continent by 2050, replacing fossil fuels with renewable energy sources [1]. This transition must also accommodate a projected increase in global electricity demand of 80% to 150% by 2050 [2]. The shift to renewable energy is transforming the electricity sector into micro-decentralized interconnected grids [3]. Variable customer behavior and the intermittent nature of renewable generation create significant challenges, such as frequency variation and voltage regulation [4]. To meet this dynamic demand, system operators must balance generation and schedule power units effectively, a task generally solved by the SCUC problem, which optimizes power generation scheduling while considering grid security, reliability, and economic factors [5].

The SCUC problem is formulated as a Mixed Integer Linear Programming (MILP), including binary variables for generator status and continuous variables for power and energy balance constraints. The problem complexity is increased by the deterministic N-1 approach, ensuring grid security by considering all the potential failures. As generation units increase, centralized algorithms may struggle with calculation complexity, scalability, and solution time [6].

Several previous works have achieved significant scientific advancements to address the computational challenges presented by the existing SCUC algorithms and accelerate the problem-solving process. Among these, Decomposition is an effective simplification approach for solving complex SCUC problems [7]. It involves breaking them into smaller, more manageable sub-problems. Three well-known decomposition approaches for SCUC are Domain Decomposition [8], Time Decomposition [9], [10], and Spatial Decomposition [11], [12].

Our approach focuses on Spatial Decomposition, a relatively less explored area where the complexity of the SCUC problem is reduced by dividing the grid into multiple areas. Each area is managed as a local SCUC sub-problem in parallel, with the overall problem solved iteratively and coordinated using ADMM [13]. We also utilize consensus ADMM to address system reserve sharing and employ the admittance matrix to establish relationships between power injection and voltage phase angles at the borders of each area. Additionally, our method incorporates BESS with temporal linking constraints and binary variables for charging, discharging, and load demand constraints (connected or disconnected), which are crucial for today's energy markets.

The paper is structured as follows: Section II formulates the deterministic SCUC problem, Section III details the proposed Spatially Decomposed Security-Constrained Unit Commitment (D-SCUC) methodology, Section IV presents numerical test results, and Section V covers conclusions and future work.

II. Security Constrained Unit Commitment Formulation

In this study, the SCUC problem uses a modified formulation from [14]. The subsequent subsections will briefly outline the objective function (cost) and constraints associated with SCUC formulations.

A. Objective Function

In an electricity market with grid-connected storage, the objective of SCUC is to minimize the generation cost (1). Fixed costs, variable costs, start-up costs, shut-down costs, reserve-up costs, and reserve-down costs contribute to the total generation cost. In a market context, maximizing social welfare requires minimizing the discrepancy between generation and load demand, leading to associated costs for demands. For

simplification, the BESS capital or fixed costs are ignored, and only the spot market prices for charging and discharging are considered.

$$\min \sum_t \left(\sum_g C_g(P_{g,t}) + \sum_b C_{bd}(P_{bd,t}) \right) - \left(\sum_b C_{bc}(P_{bc,t}) + \sum_d C_d(P_{d,t}) \right) \ \forall g, d, b, t \tag{1}$$

Where $C_g(P_{g,t})$ represents the generation cost for unit g at time t, $C_{bd}(P_{bd,t})$ reflects the cost associated with BESS discharging, $C_{bc}(P_{bc,t})$ indicates the cost of BESS charging, and $C_d(P_{d,t})$ represents the cost of serving load demand d. The variables $P_{g,t}$, $P_{d,t}$, $P_{bc,t}$, and $P_{bd,t}$ denote the active power for generation, load demand, BESS charging, and BESS discharging, respectively, for each time step t. In this formulation, all costs are modeled as stepwise functions to accurately capture the complexities of market scenarios.

B. Technical Constraints

The SCUC problem is subjected to the constraints of the generator, demand, reserve, power balance, battery storage, and the grid.

(a) Power Balance Constraints

$$\sum_g P_{g,t} + \sum_b P_{bd,t} = \sum_d P_{d,t} + \sum_b P_{bc,t} \ \forall g, d, b, t \tag{2}$$

(b) Ramping Up/Down Constraints

$$RS_g^{up} + P_{g,t} - P_{g,t-1} \le R_g^{up} + (P_g^{\min} - R_g^{up}) \cdot y_t \quad \forall g, t \ge 2 \tag{3a}$$

$$RS_g^{dw} + P_{g,t-1} - P_{g,t} \le R_g^{dw} + (P_g^{\min} - R_g^{dw}) \cdot z_t \quad \forall g, t \ge 2 \tag{3b}$$

where R_g^{up}, R_g^{dw} RS_g^{up} and RS_g^{dw} are ramp-up (3a), ramp-down (3b), upward and downward reserve capacities. $P_g^{\min}$, $P_{g,t}$ and $P_{g,t-1}$ are the allowed minimum power output of the generator, generating power output at time *t* and *t-1*. y_t and z_t are the status of the generator for start and shutdown, respectively.

(c) Power Bounds

$$P_g^{\min} \cdot u_{g,t} \le P_{g,t} \le P_g^{\max} \cdot u_{g,t} \ \forall g, t \tag{4}$$

where P_g^{max} is the maximum output power of generating unit *g*, $u_{g,t}$ is the generator status (ON/OFF) at time t.

(d) Reserve Limits

$$RS_g^{up} + P_{g,t} \le P_g^{\max} \cdot u_{g,t} \ \forall g, t \tag{5a}$$

$$RS_g^{dw} \le P_{g,t} - P_g^{\min} \cdot u_{g,t} \ \forall g, t \tag{5b}$$

(e) Minimum Up/Down Time Constraints

$$\sum_g y_{g,\tau} \le u_{g,t};\ \tau = \max(1, t - T_g^{on} + 1) \ \forall g, t \tag{6a}$$

$$\sum_g z_{g,\tau} \le 1 - u_{g,t};\ \tau = \max(1, t - T_g^{off} + 1) \ \forall g, t \tag{6b}$$

where T^{on} and T^{off} are the minimum ON time and OFF time of generating unit *g*.

(f) Start-Up and Shut-Down Constraints

$$y_{gt} - z_{gt} = u_{gt} - u_{g(t-1)} \ \forall g, t \tag{7a}$$

$$y_{g,t} + z_{g,t} \le 1 \ \forall g, t \tag{7b}$$

(g) Load Demand Constraints

$$0 \le P_{d,t} \le Pd_{d,t}^{max} \ \forall t, d \tag{8}$$

where $P_{d,t}$ and $Pd_{d,t}^{max}$ are the power of demand and maximum demand for every demand unit *d* for all time steps *t*.

(h) Power Reserve Constraints

$$\sum_t RS_g^{up} \ge \sum_d P_{d,t} \cdot R_{margin} \ \forall g, d, t \tag{9a}$$

$$\sum_t RS_g^{dw} \ge \sum_d P_{d,t} \cdot R_{margin} \ \forall g, d, t \tag{9b}$$

where R_{margin} is the reserve margin between [0, 1].

(i) Energy to Power Balance Constraints

$$\Delta t(P_{bc,t} \cdot \eta_{ch} - P_{bd,t}/\eta_{dc}) = SoC_{b,t} - SoC_{b,t-1} \ \forall b, t \tag{10}$$

where $P_{bc,t}$ and $P_{bd,t}$ are the BESS charge and discharge power, η_{ch} and η_{dc} are the efficiencies of charging and discharging. $SoC_{b,t}$ and $SoC_{b,t-1}$ are the state of charge of the BESS at time *t* and *t-1*. Δt is a constant defined for power-to-energy conversion (e.g., Δt= 1 for hour, and Δt= 0.5 for 30 minutes).

(j) BESS Charge/Discharge Constraints

$$P_{bc,t} + m_{b,t} \cdot P_{b,t}^{Cmax} \le P_{b,t}^{Cmax} \ \forall b, t \tag{11a}$$

$$P_{bd,t} - m_{b,t} \cdot P_{b,t}^{Dmax} \le 0 \ \forall b, t \tag{11b}$$

where $P_{b,t}^{Cmax}$ and $P_{b,t}^{Dmax}$ are the maximum charging and discharging power of BESS. m_t is a binary variable that represents the state (ON / OFF) of the BESS.

(k) Transmission Line Capacity Constraints

To efficiently model transmission capacity constraints, this study employs linear power flow equations (DC power flow), which offer a good approximation of non-linear power flow equations (AC power flow) [15]. The use of linear power flow equations allows the possibility of using Linear Sensitivity Factors (LSF) [16], [17], enabling the formulation of active power flow using the Power Transfer Distribution Factor (PTDF) [18]. PTDF explains the change in power flow when power injection changes from one bus to another. Furthermore, N-1 security constraints are modeled using the Line Outage Distribution Factor (LODF) which quantifies the change of power on each line after an outage of a line has occurred [19]. Transmission constraints are given in (12).

$$-f^{\max} \le [\mathrm{ptdf_u}]_l \cdot \bar{P}_u \le f^{\max} \quad \forall u \in g, b, d \tag{12}$$

where $[\mathrm{ptdf_u}]_l$ is the PTDF row related to the branch l with equivalent connected units (generator, BESS, and

demand) and $\bar{P}_u$ is the column vector related to the injected power from units. $f^{\max}$ is the maximum allowable power flow on each branch.

(l) N-1 Security constraints

Security constraints are set to cover up unplanned outages of a transmission line (N-1 case). Using the LODF, the post-contingency constraints are formulated as in (13).

$$\begin{aligned} -f^{\max} &\leq \left([\mathrm{ptdf}_u]_l + \mathrm{lodf}_{k,l}\,[\mathrm{ptdf}_u]_k\right)\bar{P}_u \\ &\leq f^{\max} \quad \forall u \in \{g,b,d\} \end{aligned} \tag{13}$$

where $lodf_{k,l}$ is the LODF row related to the line l due to the outage in the line k. This study does not consider generator outages; instead, LODF is utilized to adjust the pre-contingency PTDF to derive updated PTDFs for the post-contingency of the grid.

III. Spatially Decomposed Security Constrained Unit Commitment Formulation

The algorithm shown in Fig.1 works as follows. The D-SCUC approach begins by decomposing the grid into several areas. Each area then formulates its own independent local SCUC problem, which can be solved in parallel. The boundaries of each area are coordinated with the central coordinator using ADMM, facilitating the sharing of limited information to solve the entire SCUC problem. This iteration continues until the stopping condition is met. Once the ADMM process stops, the central coordinator, employing consensus with regularization, transmits information from the sub-models to the rebuilt the holistic model. This information includes fixed generator binary values (ON/OFF) and violated network constraints. Subsequently, the holistic model transforms the SCUC problem from MILP into a simpler Linear Programming (LP) problem, which is easier to solve. Moreover, depending on the feasibility of the solutions, the generator binary values may be relaxed if deemed necessary. The following subsection explains each step in the modeling of the D-SCUC.

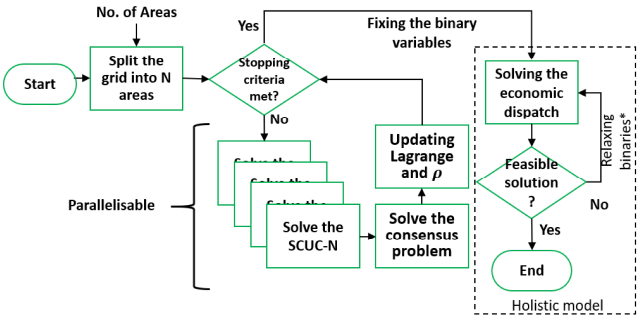

Fig. 1. Proposed Spatial Decomposed SCUC Method

A. Grid Partition Using METIS

Grid decomposition is the first step in D-SCUC. METIS is used to achieve this, as it is a powerful open-source software package to partition large irregular graphs and mesh partitioning [20]. METIS is chosen for this study because it can improve the efficiency of the parallel algorithm by keeping the number of controllable devices (generators, BESS, etc.) in each area as equal as possible with a minimum number of tie-lines between areas. Similar-sized areas are created by assigning additional weighting to buses connected to generators, BESS units, and parallel lines between the same buses.

B. Iterative SCUC Approach

The SCUC methodology is computationally expensive, as it needs to solve a number of transmission and security constraints ($2 \cdot N_{timesteps} \cdot N^2_{branches}$) [21]. To improve computational efficiency, an iterative approach is used to include security and potential network constraints in the SCUC problem. In the iterative approach, see Fig.2, the SCUC problem is first solved without transmission power flows and N-1 security constraints. After the first iteration, the power flows for each branch are calculated, and the most significant violated constraints are added to the model iteratively. The iterative process is repeated until the maximum number of iterations is reached or until there are zero net violations.

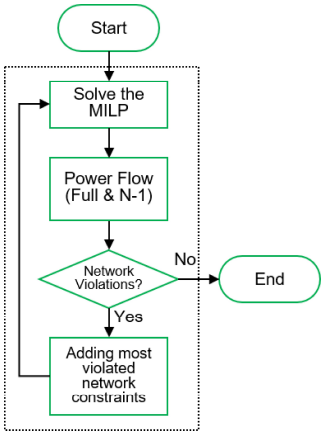

Fig. 2. Iterative addition of violated network constraints into SCUC

C. Multi Area Coordination Using ADMM

The concept and formulation of ADMM are based on Boyd's work [22] and the generalized form is adjusted in the subsequent sections to match the formulation of the D-SCUC. The mathematical formulation of the coordination of D-SCUC using ADMM is similar to that of the Centralised SCUC (C-SCUC) (see section II). In addition to information about grid assets within their respective areas, boundary information between neighboring areas are necessary for formulating the D-SCUC model.

(a) Modeling of Electrical Boundaries

Each area in a multi-area system is interconnected through tie lines, implying interdependence in their constraints and objective functions. Decoupling is achieved by introducing a virtual bus in the middle of each tie line, effectively splitting the line into two with half the reactance of the original. The electrical balance is maintained by accounting for the information about the

power p (14a) and the phase angle θ (14b) of the buses connected through tie lines. Using LSF, the border power p_b and the border phase angle θ_b can be linked to the generation or load demand p_i through a set of equality constraints, without explicitly including θ_i in the formulation (15). This approach assumes a higher number of internal buses than border buses, which replaces traditional power balance constraints at the border. y_{bb}, y_{ii}, and y_{bi} denote the self-admittance of border areas, internal areas, and admittance between internal and border areas, respectively.

$$\mathrm{p}_{\text{left}} + \mathrm{p}_{\text{right}} = 0 \tag{14a}$$

$$\theta_{\text{left}} = \theta_{\text{right}} \tag{14b}$$

$$\begin{gathered} \begin{bmatrix} p_i \\ p_b \end{bmatrix} = \begin{bmatrix} y_{ii} & y_{ib} \\ y_{bi} & y_{bb} \end{bmatrix} \begin{bmatrix} \theta_i \\ \theta_b \end{bmatrix} \\ \left(y_{bi} y_{ii}^{-1}\right) p_i + \left(y_{bb} - y_{bi} y_{ii}^{-1} y_{ib}\right) \theta_b - I p_b = 0 \end{gathered} \tag{15}$$

(b) Solving the System Constraints
Spatial decomposition uniquely addresses system constraints, such as spinning reserves, by introducing shared variables for upward and downward reserves at each time step. These variables play a crucial role in the regularization phase of the consensus problem, which is integral for solving the central problem.

(c) Inter-area N-1 Constraints
Inter-area network outages occur when a line outage in one area triggers a contingency in other area. These inter-area violations are typically not explicitly modeled as variables between areas, making the modeling of inter-area N-1 constraints challenging. Consequently, the violations resulting from inter-area outages are addressed in the post-processing stage following the ADMM steps.

(d) Binary variables in the D-SCUC model
The SCUC problem involves a mix of continuous and binary variables, making it a non-convex optimization problem. ADMM, typically applied to convex optimization problems involving continuous variables, faces limitations in handling non-convexity. In D-SCUC using ADMM, we approximate the impact of binary variables as continuous to a certain extent. This approximation allows ADMM to achieve linear convergence, even with a large number of binary variables treated as shared variables. This approach assumes that the electrical quantities at the borders (such as power and phase angle) are sufficiently smooth and minimally affected by nonlinearities.

(e) Objective Function in D-SCUC
In ADMM-based D-SCUC, we have two objective functions. The first is the normal MILP-based objective function of each area (1), and the second is the Augmented Lagrangian objective function from the boundaries (16).

$$\min \sum_{a=1}^{A} \{(\lambda \cdot [X - Z] + \frac{\rho}{2} \cdot X^2 - \rho[X \cdot Z])\} \tag{16}$$

where A is the total number of areas. λ, X, Z, and ρ represent the Lagrangian multiplier, the shared border variable, the dual variable, and the ADMM weighting factor, respectively (for power, phase angle, reserve-up and reserve-down). The resulting objective function for each area in the D-SCUC is the summation of equation (1) and equations (16).

(f) Modified Power Balance Constraints of D-SCUC
The power balance constraints are modified by including the border power information see (17).

$$\sum_{g} P_g + \sum_{b} (P_{bd} - P_{bc}) - \sum_{d} P_d + \sum_{x} f_{dir} \cdot X_p = 0 \tag{17}$$

where X_p denotes the shared power ($X_p > 0$) and f_{dir} is the direction of power flow, ($f_{dir} \in \{-1, +1\}$).

(g) Modified Network and Security Constraints
The network constraints (12) and the N-1 security constraints (13) are further improved by including the power flow direction f_{dir} at the boundary buses.

D. ADMM Central Coordinator

The central coordinator in the distributed ADMM is responsible for coordinating sub-area problems and updating their parameters. While boundary information is shared among the sub-areas, it's important to note that no sensitive data is exchanged with the central coordinator.

(a) ADMM Central Objective Function
The central coordinator formulates objective functions using the shared border values from each area. The power X_p and phase angle X_θ between the area is shared between each tie-line (area on the left *tl* and right (*tl+1*) of each tie-line. This leads to the generalized form of the quadratic objective function of power and phase angle (18).

$$\begin{gathered} \sum_{a=1}^{A} \left(-\lambda \cdot Z_{+} \frac{\rho}{2} \cdot X - Z^2\right) + \\ \left(-\lambda \cdot Z_{tl+1} + \frac{\rho}{2} \cdot X_{tl+1} - Z^2\right) \end{gathered} \tag{18}$$

The generalized objective function for the reserve capacity (upward and downward) is created for each area, not from the tie lines (19).

$$\sum_{a=1}^{A} (-\lambda \cdot Z + \frac{\rho}{2} \cdot X) - Z^2) \tag{19}$$

The final central objective function is the summation of the objective function for power, phase angle, reserve-up, and reserve-down.

(b) Updating Lagrangian Multiplier
Once the central objective problem is solved and Z is updated for power, phase, upward and downward reserve, the Lagrangian multiplier λ is updated accordingly (20) and is sent back to each area to solve their local SCUC again.

$$\lambda^{+} = \lambda + [\rho] \cdot [X - Z] \tag{20}$$

(c) ADMM Based Distributed Algorithm
The steps for solving the D-SCUC using ADMM are presented as pseudo-code in Algorithm.1.

Algorithm 1 ADMM Based D-SCUC

Require: 1. Initialise ρ, λ, X, Z for all areas.
2. Each area solves its SCUC independently and in parallel
3. Area sends X to the central coordinator.
4. The central coordinator solves the central problem (18,19).
5. The coordinator then sends the updated Z to areas.
if Stopping criteria satisfied (III-F) **then**
6. Stop.
else
6. The areas solve SCUC again by updating λ (20) and ρ (Algorithm2) and repeat from step 2.
end if

E. Dynamic Weighting Factor

In ADMM, the initial weighting factor (ρ) is critical; a well-tuned value can significantly enhance convergence speed and solution quality, while a poorly chosen one may lead to slow convergence or even divergence [22]. The optimal ρ value is typically determined through a pilot run for each test grid and area configuration, a process that can be time-consuming. To prevent oscillation and premature convergence, ρ is adjusted based on the orders of the primal and dual residuals, with their calculations outlined in (21a) - (21b). The additional border weighting W is determined by ρ, with parameters μ, ρ^+, and ρ^- defining the starting value, increment, and decrement rates, respectively. The pseudo-code for updating the dynamic weighting factor W in ADMM is presented in Algorithm 2.

$$prim = 2 \cdot (X_{tl} - X_{tl+l})^2 \quad \forall t, areas \tag{21a}$$

$$dual = W^2 \cdot (Z_t - Z_{t-1})^2 \quad \forall t, areas \tag{21b}$$

Algorithm 2 Update of dynamic weighting factor

Require: Initialize $\rho, W, \mu, \rho^+, \rho^-$
while stopping criteria are not met **do**
After each ADMM iteration, get *prim* and *dual* for P and θ.
if $P_{prim} > \mu \cdot P_{dual}$ **then**
$W_P^+ = W_P \cdot \rho^+$ **and** $\rho_P = \rho_P \cdot \rho^+$.
else if $P_{dual} > \mu \cdot P_{prim}$ **then**
$W_P^+ = W_P / \rho^-$ **and** $\rho_P = \rho_P / \rho^-$.
end if
if $\theta_{prim} > \mu \cdot \theta_{dual}$ **then**
$W_\theta^+ = W_\theta \cdot \rho^+$ **and** $\rho_\theta = \rho_\theta \cdot \rho^+$.
else if $\theta_{dual} > \mu \cdot \theta_{prim}$ **then**
$W_\theta^+ = W_\theta / \rho^-$ **and** $\rho_\theta = \rho_\theta / \rho^-$.
end if
end while

F. ADMM Stopping Criteria

Defining stopping criteria is crucial to balancing optimality and speed. The following conditions must be met to satisfy the stopping criteria and either of them needs to be satisfied:

- The system imbalance per load ($\left(\frac{Pg+Pd+PBESS}{Pd}\right) \cdot 100$) is required to be less than the threshold (user-defined) for each time step.
- The generator status (ON/OFF) remains the same through two adjacent iterations ($u_{g,t} = u_{g,t-1}$).
- Primal and dual values for power and phase angle between the tie-line is less than the threshold (user-defined).
- The current iteration is equal to the maximum number of ADMM iterations (user-defined).

G. Rebuilding the Holistic Model

The process of reconstructing the holistic model aims to fine-tune SCUC solutions from all areas. This process involves identifying all the inter-area network constraints from the D-SCUC models. Here, ADMM is used to fix the generator binaries, thus offering a warm start for rebuilding the holistic model. Binaries are relaxed if the solution is found to be infeasible. Once reconstructed, the violated network constraints from the decomposed approach are systematically added, along with security constraints like inter-area N-1 constraints, into the problem. The rebuilt holistic model takes the form of an LP problem for solving economic dispatch and is straightforward to solve.

IV. Numerical Test Results

The spatial-based decomposition method was tested on the IEEE-118 [23] and RTE-6468 [24] grids under 25 scenarios for each, combining 5 daily demand and 5 generation bids over 24 hours. The tests were carried out on a Linux Mint 20.2 system with an AMD Ryzen 9 3950X CPU, 128 GB RAM, and using Julia with the JuMP package [25]. All subproblems are solved in parallel by exploring the parallelization possibilities of Julia [26]. For solving mixed-integer (quadratic) problems, GUROBI 9.5.2 was used, configured with a MIP gap of 1%, a threshold commonly adopted in industrial applications, while IPOPT 3.14 was used to solve quadratic problems.

A. Test Setup

The rationale behind the test is to evaluate the quality of our decomposed approach in terms of *speed-up* (ratio of the time required by a C-SCUC to the time required by a D-SCUC to solve the same problem) and *optimality gap* (percentage difference between the objective function value of C-SCUC and D-SCUC) under different stopping criteria. An optimality gap of less than 0 means that the decomposed solution is more optimal (cheaper) than the holistic solution, and vice versa.

B. IEEE 118 Bus System

The IEEE 118 bus system is modified to form a test network comprising 118 buses, 18 generators, 13 BESS, 99 load demand, and 186 branches.

Optimality and Speed-up with Areas:

Fig. 3 illustrates the distribution of optimality gap and speed-up across varying numbers of areas (2, 3, 5, 10). As the number of tie lines increases from 10 (2 areas) to 12 (3 areas), 27 (5 areas), and 45 (10 areas), the average optimality gap also

increases from 0.34% to 1.06%. Concurrently, the speed-up improves with the increase in the tie lines. This improvement is due to the reduced size and complexity of SCUC sub-problems as the number of areas increases. The test results for the IEEE-118 network are summarized in Table I. However, based on these results, the centralized algorithm shows superior speed-up on the decomposed IEEE-118 bus grid (stopping criterion: normalized system balance = 0.25 pu). Therefore, D-SCUC may not be recommended for smaller networks. Cases with an optimality gap less than zero are primarily influenced by the solver tolerance of D-SCUC and the more relaxed cost values.

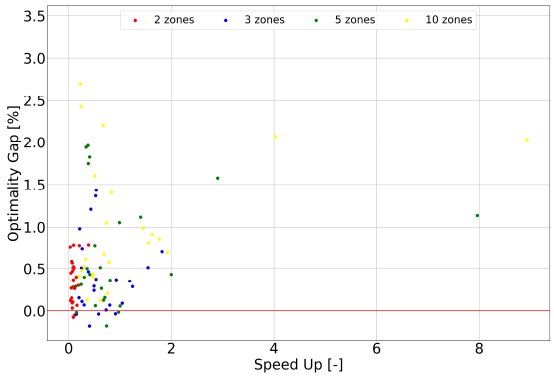

Fig. 3. Optimality gap and speed-up trend of IEEE 118 network

TABLE I
IEEE 118 NETWORK: COMPUTATIONAL RESULTS SUMMARY

Type of SCUC	No. of areas	No. of tie lines	Avg.Opt gap (%)	Avg.Speed-up
C-SCUC	1	0	0	1
D-SCUC	2	10	0.34	0.11
D-SCUC	3	12	0.38	0.62
D-SCUC	5	27	0.64	0.98
D-SCUC	10	45	1.06	1.20

C. RTE 6468 Bus System

The modified 6468-bus system consists of 6468 buses, 1186 generators, 100 BESS, 3314 load demands, and 9000 branches.

Optimality and Speed-up with Areas:

The test results of the RTE-6468 system under varying numbers of decomposed areas (100, 200, 300) are summarized in Table II. Although D-SCUC shows faster execution compared to C-SCUC, it is important to note that the average optimality gap increases gradually with an increase in the number of areas (and tie lines). Increasing ADMM iterations from 20 to 40 (for 200 areas) in the decomposed algorithm resulted in a significant decrease in the average optimality gap from 3.11% to 2.06%. However, this enhancement comes at the cost of reducing the speed-up from 5.7 to 3.77 times. Fig. 4 illustrates the distribution of the optimality gap and the speed-up under different areas. In summary, D-SCUC offers substantial speed-up for larger networks with a trade-off in optimality. *Objective Function and ADMM Iterations:*

TABLE II
RTE 6468 NETWORK: COMPUTATIONAL RESULTS SUMMARY

Type of SCUC	No. of area	No. of tie lines	Avg.Opt gap (%)	Avg.Speed-up	ADMM iter
C-SCUC	1	0	0	1	0
D-SCUC	100	970	2.95	4.79	20
D-SCUC	200	1272	3.11	5.71	20
D-SCUC	200	1272	2.06	3.77	40
D-SCUC	300	1510	3.67	5.90	20

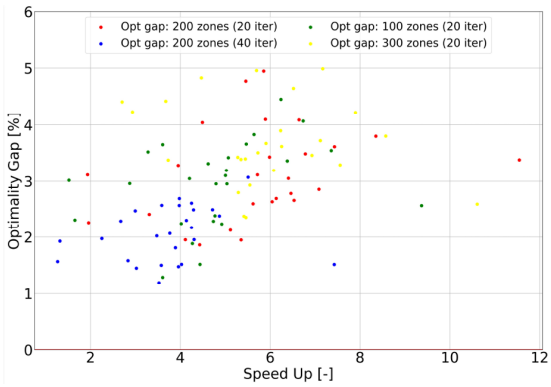

Fig. 4. Optimality gap with the speed-up of RTE 6468 network

Fig.5 shows the behavior of the RTE 6468-bus system's percentage of the objective function value (decomposed to the holistic) with ADMM iteration for different areas. It is visible

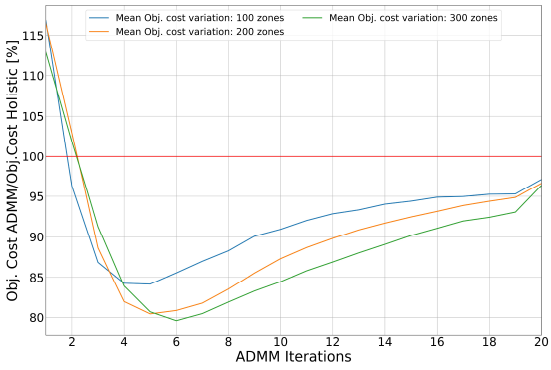

Fig. 5. Objective function with ADMM iteration for RTE 6468 Network

that the decomposed objective function value approaches the holistic objective function value (red line) over time as the ADMM iterations progress (until the 19th iteration), but it never reaches it. This is because the holistic and decomposed model can have different supplied load demands. In the last step (the 20th iteration), the holistic model is rebuilt and solved as a simple LP problem.

Generator Binaries and ADMM Iterations:

Fig.6 shows how the percentage of binary variables for generators (averaged over 25 cases) changes their values between consecutive ADMM iterations ($u_{g,t} \neq u_{g,t-1}$) across various area configurations. Notably, after approximately 10 iterations, the rate of change in these binary variables stabilizes. This observation suggests that ADMM effectively initializes with

stable binary variables, giving a robust starting point for rebuilding the holistic model.

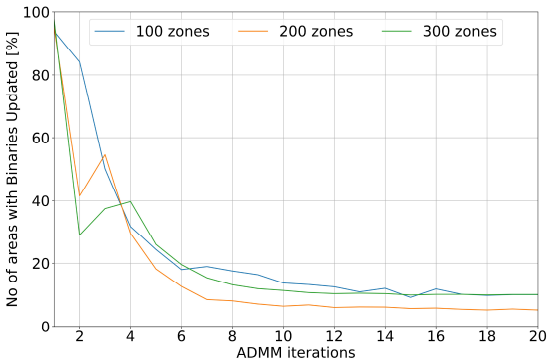

Fig. 6. Generator binaries with ADMM iterations for RTE 6468 network

V. CONCLUSIONS AND FUTURE WORK

In this work, we propose a spatially decomposed SCUC method to solve transmission and distribution grids. Our approach partitions the power system into equally weighted areas and coordinates them using ADMM to formulate the D-SCUC model. The proposed method has been formulated, tested, and validated on the IEEE 118 and RTE 6468 systems. The numerical results indicate that the decomposition method may not yield optimal results for smaller networks, but it significantly accelerates the computational speed for larger grids. This decomposition approach prioritizes speedup while accepting a compromise in optimality compared to centralized approaches. However, by fine-tuning the stopping criteria, a more favorable balance between optimality and speed can be achieved. The effectiveness of this approach depends on factors like grid partitioning strategies, stopping criteria, and the adjustment of the weighting factors.

Future work will involve dynamically updating weighting factors for all the shared variables in the D-SCUC approach and conducting a comparative analysis with various decomposition techniques of SCUC. Additionally, exploring advanced parallel computing techniques will aim to enhance computational efficiency.

REFERENCES

[1] European Commission. *European Green Deal: Striving to be the first climate-neutral continent*. 2019-12-11.

[2] IEA. *World Energy Outlook 2023*. IEA, Paris, 2023. [Online]. https://www.iea.org/reports/world-energy-outlook-2023.

[3] S. Howell ,Y. Rezgui, J. Hippolyte,B. Jayan, H. Li. *Towards the next generation of smart grids: Semantic and holonic multi-agent management of distributed energy resources*. Renewable Sustainable Energy Rev, 2017.

[4] R. Ufa, V. Rudnik, Y. Malkova, Y. Bay, and N. Kosmynina, *Impact of renewable generation unit on stability of power systems*, International Journal of Hydrogen Energy, vol. 37, 2022, Elsevier.

[5] N. Yang, Z. Dong, L. Wu, L. Zhang, X. Shen, D. Chen, Z. Daojun, B. Zhu, and Y. Liu, *A Comprehensive Review of Security-constrained Unit Commitment*, *Journal of Modern Power Systems and Clean Energy*, 2022.

[6] S. Cvijic and J. Xiong, *Security constrained unit commitment and economic dispatch through Benders decomposition: A comparative study*, IEEE Power and Energy Society General Meeting, 2011, https://doi.org/10.1109/PES.2011.6039643.

[7] A. V. Ramesh, X. Li, and K. W. Hedman, *An Accelerated-Decomposition Approach for Security-Constrained Unit Commitment With Corrective Network Reconfiguration*, *IEEE Transactions on Power Systems*, 2022.

[8] N. Taher, K. Amin and F. Farhad *A new decomposition approach for the thermal unit commitment problem*, Applied Energy, vol. 86, 2009, https://doi.org/10.1016/j.apenergy.2009.01.022.

[9] C . Mitch, F. Javad, A. Shabbir, and G. Santiago *A rolling-horizon unit commitment framework with flexible periodicity*, International Journal of Electrical Power & Energy Systems, vol-90, 2017.

[10] F. Safdarian, *Temporal Decomposition for Multi-Interval Optimization in Power Systems*, LSU Doctoral Dissertations. 5259. Aug. 2020.

[11] A. S. Xavier, F. Qiu, and S. S. Dey. *Decomposable formulation of transmission constraints for decentralized power systems optimization*, 2020.

[12] A. Kargarian, Y.Fu and Z. Li, *Distributed Security-Constrained Unit Commitment for Large-Scale Power Systems*, IEEE Transactions on Power Systems, 2015, https://doi.org/10.1109/TPWRS.2014.2360063.

[13] C. Shah, J. King and R. W. Wies, *Distributed ADMM Using Private Blockchain for Power Flow Optimization in Distribution Network With Coupled and Mixed-Integer Constraints*, in IEEE Access, 2021.

[14] A. Conejo, and L. Baringo, *Power System Operations*, 978-3-319-69406-1, 2018.

[15] M. Li, Y. Du, J. Mohammadi, C. Crozier, K. Baker, and S. Kar, *Numerical Comparisons of Linear Power Flow Approximations: Optimality, Feasibility, and Computation Time*, 2022 IEEE Power & Energy Society General Meeting (PESGM), 2022.

[16] H. Zhu, *ECE530—Analysis Techniques for Large-Scale Electrical Systems*, https://courses.engr.illinois.edu/ece530/.

[17] D. Tejada-Arango, P. Sánchez-Martın, and A. Ramos, *Security Constrained Unit Commitment Using Line Outage Distribution Factors*, IEEE Transactions on Power Systems, 2018, https://doi.org/10.1109/TPWRS.2017.2686701.

[18] M. Shahidehpour, H. Yamin, and Z. Li, *Market Operations in Electric Power Systems: Forecasting Scheduling and Risk Management*, New York, NY, USA: Wiley, 2002, https://ieeexplore.ieee.org/servlet/opac?bknumber=5201691.

[19] H. Pinto, F. Magnago, S. Brignone, O. Alsac, and B. Stott, *Security constrained unit commitment: Network modeling and solution issues*, Proc. IEEE PES Power Syst. Conf. Expo., pp. 1759-1766, 2006, https://doi.org/10.1109/PSCE.2006.296179.

[20] G. Karypis, *METIS: Unstructured graph partitioning and sparse matrix ordering system*, Technical report, Department of Computer Science, University of Minnesota, 1997.

[21] Q. Zhai, X. Guan, J. Cheng, and H. Wu, *Fast Identification of Inactive Security Constraints in SCUC Problems*, *IEEE Transactions on Power Systems*, vol. 25, no. 4, pp. 1946-1954, 2010,https://doi.org/10.1109/TPWRS.2010.2045161.

[22] S. Boyd, N.Parikh, E. Chu, B. Peleato and J. Eckstein, *Distributed Optimization and Statistical Learning via the Alternating Direction Method of Multipliers*, Foundations and Trends® in Machine learning, vol-3, 2011, https://doi.org/10.1561/2200000016.

[23] R. D. Zimmerman, C. E. Murillo-Sánchez, and R. J. Thomas, *Matpower: Steady-State Operations, Planning and Analysis Tools for Power Systems Research and Education*, Power Systems, IEEE Transactions, 2011, https://doi.org/10.1109/TPWRS.2010.2051168.

[24] C. Josz, S. Fliscounakis, J. Maeght, and P. Panciatici, *AC power flow data in MATPOWER and QCQP format: iTesla, RTE snapshots, and PEGASE* , 2016, https://doi.org/10.48550/arXiv.1603.01533.

[25] M. Lubin, O. Dowson, J. D. Garcia, J. Huchette, B. Legat, J. P. Vielma, *JuMP 1.0: Recent improvements to a modeling language for mathematical optimization*, Mathematical Programming Computation, 2023, https://doi.org/10.1007/s12532-023-00239-3.

[26] A. Edelman, *Julia: A fresh approach to parallel programming*, IEEE International Parallel and Distributed Processing Symposium, 2015, https://doi.org/10.1109/IPDPS.2015.122.